

TWO-WIND INTERACTION MODELS OF THE PROPLYDS IN THE ORION NEBULA

W. J. HENNEY AND S. J. ARTHUR

*Instituto de Astronomía, UNAM, Unidad Morelia,
J. J. Tablada 1006, 58090 Morelia, Michoacán, México*

Abstract. Many low-mass stars in the Orion nebula are associated with very compact ($\simeq 1$ arcsec) emission knots, known variously as proplyds, PIGs or LV knots. Some of these knots are teardrop-shaped, with “tails” pointing away from the massive star θ^1 Ori C, which is the principal exciting star of the nebula. We discuss models of such knots, which invoke the interaction of the fast stellar wind from θ^1 Ori C with a transonic photoevaporated flow from the surface of an accretion disk around a young low-mass star. We review previous analytic work and compare the results of the model with the observed brightnesses, morphologies and emission line profiles of the knots, as well as presenting new results from numerical hydrodynamical simulations.

1. Introduction

The proplyds are bright compact emission line knots, with sizes of order 0.5–2.0 arcseconds, that are found in the inner region of the Orion nebula (Laques and Vidal, 1979; Garay et al., 1987; Churchwell et al., 1987; Felli et al., 1993; O’Dell et al., 1993; O’Dell and Wen, 1994; McCaughrean, 1997) and nearly all of which contain an embedded low-mass star (Meaburn, 1988; McCaughrean and Stauffer, 1994). Many of the proplyds show a head/tail morphology, in which the tail points away from the star θ^1 Ori C, the most massive star of the Trapezium cluster. Emission line spectroscopy of the proplyds in the [O III] 5007Å line (Massey and Meaburn, 1993; Massey and Meaburn, 1995; Henney et al., 1997) show a bright central core with full width half maximum (FWHM) of $\simeq 50$ km s $^{-1}$, together with faint wings extending out to ≥ 100 km s $^{-1}$ from the line center.

The obvious explanation for these objects is that the radiation and stellar wind from θ^1 Ori C is interacting with the circumstellar material around the low-mass stars. In our models we assume that this circumstellar material is in the form of an optically thick, geometrically thin accretion disk. The effect of the radiation from θ^1 Ori C will be to ionize the material in the disk, which will produce a photoevaporated flow away from the disk and *towards* the ionizing source. Hence, to produce the tails pointing away from θ^1 Ori C, this flow must somehow be confined and redirected. Two possible candidates for this confinement mechanism are the exciting star's radiation pressure and the ram pressure of its stellar wind. However, only the second of these is feasible, as is shown in §2. In §3 a simple analytic model of the resultant two-wind interaction is briefly described and the successes and failures of the model in explaining observed properties of the proplyds are outlined in §4. In §5, preliminary results of numerical hydrodynamic simulations are presented, which remove some of the arbitrary assumptions of the model. Complications such as the possible existence of a neutral photodissociated flow are critically discussed in §6.

2. Confinement Mechanisms — Radiation vs. Ram Pressure

The gas pressure at the base of the ionized flow can be calculated simply by equating the numerical flux, F_0 , of Lyman continuum (Ly-c) photons arriving at the ionization front (IF) with the numerical flux of newly-ionized ions entering the photoevaporated wind:

$$F_0 = n_0 u_0 , \quad (1)$$

where n_0 is the ion number density and u_0 the ion velocity at the base of the wind. This leads to the following expression for the gas pressure

$$P_{\text{gas}} \equiv \mu m_{\text{H}} n_0 c_0^2 = \mu m_{\text{H}} c_0 F_0 / \mathcal{M}_0 , \quad (2)$$

where μ is the mean atomic mass ($\simeq 1.3$), m_{H} is the mass of hydrogen, c_0 is the sound speed in the ionized gas ($\simeq 12 \text{ km s}^{-1}$) and \mathcal{M}_0 is the Mach number at the base of the flow, which will be of order 1–2 (Dyson, 1968; Kahn, 1969; Bertoldi, 1989).

The *unattenuated* ionizing flux is given by $F_{\star} = \dot{S}_{\star} / 4\pi d^2$, where \dot{S}_{\star} is the stellar ionizing photon rate, for which estimates vary between $7 \times 10^{48} \text{ s}^{-1}$ (Panagia, 1973) and $3 \times 10^{49} \text{ s}^{-1}$ (Bertoldi and Draine, 1996), and d is the distance of the proplyd from the exciting star. However, at the distances of the proplyds from θ^1 Ori C, most of this flux is used up in maintaining the ionization state of the photoevaporated flow against recombination. With the assumption that $F_0 \ll F_{\star}$, one can write

$$F_{\star} e^{-\tau_0} = f(\tau_0) n_0^2 \alpha_{\text{B}} r_{\text{d}} , \quad (3)$$

where τ_0 is the dust absorption optical depth of the flow, α_B is the Case B recombination coefficient ($2.6 \times 10^{-13} \text{ cm}^3 \text{ s}^{-1}$), r_d is the disk radius and $f(\tau_0) \simeq (3 + \tau_0)^{-1}$ depends slightly on the assumed geometry (Henney et al., 1996). Assuming $\tau_0 = 0$, one finds (Eqs. 1 and 3) that the *percentage* of ionizing photons reaching the ionization front is

$$\beta_{\%} = \frac{100 F_0}{F_{\star}} = 1.5 \mathcal{M}_0 d_{17} r_{15}^{-1/2} \dot{S}_{49}^{-1/2}, \quad (4)$$

where d_{17} and r_{15} are the proplyd distance and disk radius measured in units of 10^{17} cm ($\simeq 0.3 \text{ pc}$) and 10^{15} cm ($\simeq 66 \text{ au}$) respectively and \dot{S}_{49} is the stellar ionizing photon rate in units of 10^{49} s^{-1} . Allowing for the effects of dust makes little difference to this estimate.

The ionizing radiation pressure from $\theta^1 \text{ Ori C}$ that acts on the photoevaporated flow can be written as

$$P_{\text{rad}} = \frac{F_{\star} \langle h\nu \rangle}{c}, \quad (5)$$

where c is the speed of light, F_{\star} is the *unattenuated* ionizing flux from $\theta^1 \text{ Ori C}$, and $\langle h\nu \rangle$ is the mean energy of ionizing photons absorbed in the flow ($\simeq 13.6 \text{ eV}$). Hence,

$$\frac{P_{\text{rad}}}{P_{\text{gas}}} \simeq \frac{h\nu_0 F_{\star} \mathcal{M}_0}{\mu m_{\text{H}} c_0 c F_0} = 0.033 \mathcal{M}_0 \beta_{\%}^{-1} = 0.022 d_{17}^{-1} r_{15}^{1/2} \dot{S}_{49}^{1/2}. \quad (6)$$

This ratio is always significantly less than unity, therefore the ionizing radiation pressure is **incapable** of confining the photoevaporated flow. If there were enough dust opacity at the base of the flow, then it is conceivable that the non-ionizing radiation from $\theta^1 \text{ Ori C}$ (FUV, optical) may make a significant contribution to the radiation pressure. However, the bolometric luminosity of $\theta^1 \text{ Ori C}$ is only ~ 3 times its Ly-c luminosity, so the above conclusion is unchanged and radiation pressure falls an order of magnitude short of the thermal pressure even for the closest proplyds ($d_{17} \simeq 0.5$).

Turning now to the ram pressure, P_{hyd} , of the stellar wind from $\theta^1 \text{ Ori C}$, this will be given by

$$P_{\text{hyd}} = \rho_w v_w^2, \quad (7)$$

where ρ_w and v_w are respectively the stellar wind density and velocity. Since the wind is radiation-driven, one would expect the ratio $P_{\text{hyd}}/P_{\text{rad}}$ to be of order unity and, using the observed parameters of $\theta^1 \text{ Ori C}$ (Howarth and Prinja, 1989; Panagia, 1973), one finds (Henney et al., 1996) that this is indeed the case. However, although the radiation pressure must act on the base of the wind where the majority of the recombinations occur, the ram pressure need not do so, but will act on the surface of contact between

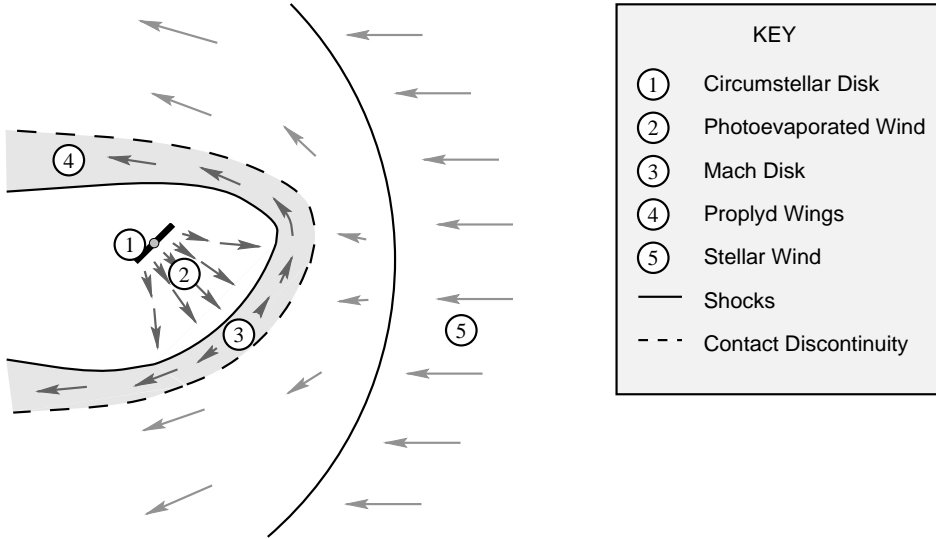


Figure 1. Schematic diagram of the two-wind interaction model. Ionizing photons from θ^1 Ori C drive a photoevaporated wind from one face of the circumstellar disk, which interacts supersonically with θ^1 Ori C's stellar wind.

the evaporated flow and the stellar wind, wherever that may be. Hence, the photoevaporated gas will flow divergently away from the disk until its pressure (reduced by geometric dilution) falls to that of P_{hyd} , at which point it can be confined by the stellar wind.

3. Analytic Two-Wind Models

The analytic model (Henney et al., 1996) depends chiefly on the dimensionless parameter $\lambda \equiv P_{\text{gas}}/P_{\text{hyd}}$. From the discussion of the previous section, it is evident that $\lambda > 1$, in which case the photoevaporated flow, which is initially mildly supersonic (Dyson, 1968; Kahn, 1969; Bertoldi, 1989), will begin to flow freely away from the disk. It is assumed that the streamlines are straight and that the initial flow diverges with a half-opening angle of 45° . If the velocity remained constant, the density would fall as $(1+z)^{-2}$, where z is the height above the disk in units of the disk radius, but a pressure gradient causes the flow to accelerate.

The flow will shock at the point where its pressure has fallen to that of P_{hyd} , which occurs at a distance

$$D \simeq \frac{1.19 (\ln \lambda)^{1/4} \lambda^{1/2}}{\cos^2 \theta_0} r_d = 4-20 r_d , \quad (8)$$

where θ_0 is the inclination angle of the disk normal with respect to the direction to θ^1 Ori C and, for the second equality, $\lambda = 10\text{--}100$ is assumed. The shock will be radiative, so can be treated as isothermal, although the radiation from the shock itself makes a negligible contribution to the proplyd luminosity. A shock will also form in the wind from θ^1 Ori C, but this will be non-radiative, hence the assumption of ram pressure balance used to derive equation 8 is not strictly valid (see § 5).

A thin, almost flat, layer (Mach disk) of shocked photoevaporated flow material forms parallel to the circumstellar disk and gas flows outwards along this layer, reaching a velocity at the edge of

$$v_\ell \simeq 3.8(\ln \lambda)^{1/2} c_0 = 70\text{--}100 \text{ km s}^{-1}. \quad (9)$$

The gas is then swept back by the wind of θ^1 Ori C to form the proplyd wings and tail. Figure 1 illustrates the components of the model in a schematic form.

For reasonable values of λ , the photoevaporated disk wind is the brightest component of the model (with a luminosity $\simeq 0.5\lambda^{1/2}$ times that of the Mach disk plus tail) and also the smallest, leading to a core-halo morphology (Henney et al., 1996, Fig. 11).

4. Comparison with Observations

The ensemble properties of the proplyds are quite well reproduced by the analytic model. The models show good agreement with the observed trends of proplyd size and luminosity vs. distance from θ^1 Ori C, the former increasing and the latter decreasing (McCullough et al., 1995; Henney et al., 1996, Figs. 9 and 10). The implied circumstellar disk radii are between 20 and 60 au ($r_{15} \simeq 0.3\text{--}1.0$). These correlations, however, are rather insensitive to the details of the model.

The morphologies of individual proplyds are compared with model predictions in Figure 2 (a larger sample is given in Fig. 14 of Henney et al., 1996), where it can be seen that the models successfully reproduce single and double tails, both of which are observed (O'Dell and Wen, 1994; O'Dell and Wong, 1996; Johnstone et al., 1996). However, the double tails may be merely the result of absorption in the core of the tail, which is not consistent with the models as they stand. The crescent head observed in many proplyds would correspond to the Mach disk in the models, but this is rather problematic since the models predict that this should be less bright than the photoevaporated wind component (§ 3), which is not the case for most proplyds, although dust absorption at the base of the wind ($\tau \simeq 0.5\text{--}1$ for the closest proplyds) would alleviate this problem (this is included in the fit to OW 158–327).

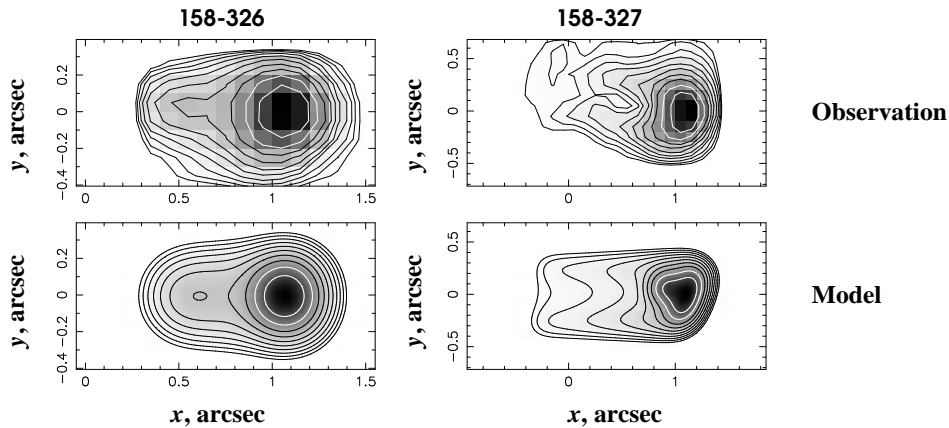


Figure 2. Comparison of morphological predictions of the two-wind interaction model with observations. Contours and greyscales show $H\alpha$ surface brightness (logarithmic scale) for *HST* observations and model images. The interval between successive contours is $2^{1/2}$.

Detailed comparisons between model predictions and high resolution $[O\text{ III}]$ 5007\AA spectra of individual proplyds are presented in Henney et al. (1997). The evaporated wind produces the bright core of the line, with width of a few times the sound speed in the ionized gas, while the Mach disk and tail produce the high-velocity line wings that are observed. However, in order to reproduce the $\simeq 100\text{ km s}^{-1}$ widths of the line wings seen in LV 5 (OW 158–323) and LV 2 (OW 167–317), values of $\lambda = 50\text{--}200$ are required, which are 3–4 times larger than those found in fitting the morphologies of the same objects (Henney et al., 1996).

5. Hydrodynamical Simulations

Figure 3 shows the results of an example numerical simulation of the two-wind interaction (Henney and Arthur, 1997). In this simulation, the circumstellar disk (oriented vertically in the figure) is inclined by 45° with respect to the direction of the stellar wind from θ^1 Ori C (other parameters are described in the figure caption). The transfer of ionizing radiation in the photoevaporated flow is not calculated self-consistently in the models, but the boundary conditions are assumed constant over the disk surface and are taken from the analytic model. Also, the simulation parameters correspond to a rather small value of λ ($\simeq 8$), since a larger value would require an unfeasibly large computational grid.

The main differences with respect to the analytic calculation are due to the relaxation of two arbitrary assumptions of the model. Firstly, the pho-

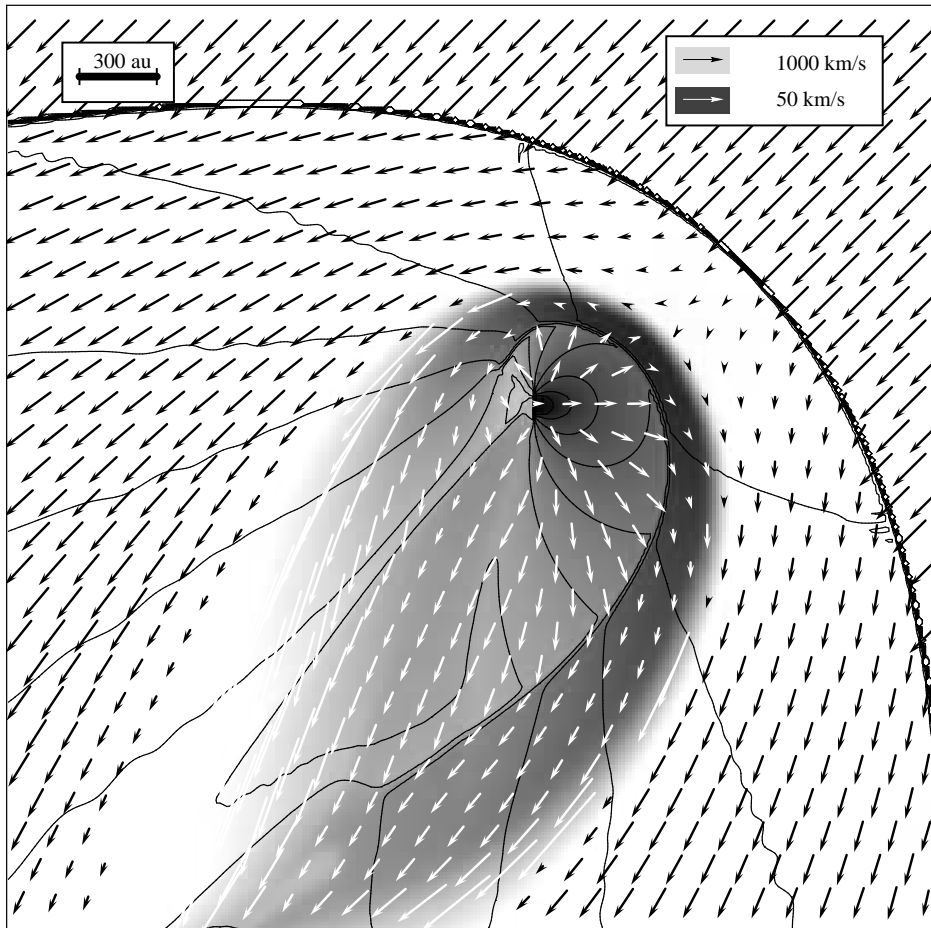


Figure 3. Hydrodynamical simulation of the two-wind interaction, calculated in 2D slab symmetry with a grid size of 300×300 cells. Greyscale shows the gas density while contours show the gas pressure (both logarithmic scale). Arrows show gas velocity. Photoevaporated disk material (white arrows) has an isothermal equation of state. Stellar wind material (black arrows) has an adiabatic equation of state. Note the different velocity normalizations of the black and white arrow lengths. The parameters of the model are $r_d = 30$ au, $\theta_0 = 45^\circ$, $n_0 = 2 \times 10^5 \text{ cm}^{-3}$, $n_w = 1 \text{ cm}^{-3}$, $u_w = 1000 \text{ km s}^{-1}$.

toevaporated flow is calculated self-consistently, instead of being assumed to follow straight streamlines with opening angle 45° . Pressure gradients in the mildly supersonic wind in fact cause the flow to diverge increasingly with distance from the disk. Secondly, the (non-radiative) shock in the stellar wind is treated properly, instead of merely assuming ram pressure balance between the two winds as was done in the analytic model. Both these factors affect the shape of the dense layer of shocked photoevaporated

wind material, which is more curved than in the analytic calculation. The flat “Mach disk” of the analytic model is no longer apparent and there is no sharp distinction between the Mach disk and tail. The gas velocities reached in the shocked photoevaporated wind are also slightly smaller than in the analytic model. Unfortunately, the use of slab symmetry, which allows the asymmetric interaction to be modelled in two dimensions, means that it is not possible to produce emission maps or spectra from the simulations. Nonetheless, the morphology and kinematics of the simulations are rather similar to those of the analytic calculation modulo the differences noted above. The arguments for and against the two-wind interaction model are hence little affected.

6. Discussion and Speculation

Despite the success of the two-wind interaction models in reproducing the observed morphologies and kinematics of the proplyds, some problems remain. In particular, the apparent absorption in the tails of some objects and the [O III]/IR arcs (Bally et al., 1995; Hayward et al., 1994) that are seen between the closer proplyds and θ^1 Ori C are both hard to explain with the two-wind model. An alternative view (Bally et al., 1995; Johnstone et al., 1996) is that the disk evaporation is controlled by non-ionizing FUV photons, with the ionization front occurring away from the disk. The proplyd morphology would then be determined by the shape of the ionization front. The hydrodynamic interaction with the stellar wind from θ^1 Ori C would, on this view, still occur, but farther out in the flow, perhaps producing the [O III]/IR arcs. This model has had most success in explaining the characteristics of HST 10 (OW 182–413), but this object does not seem to be typical of proplyds as a class (in particular, its tail does not point exactly away from θ^1 Ori C and it may not contain a central star). Johnstone et al. (1996) compare the mass-loss rates from photodissociated and photoionized disk winds and conclude that the former will dominate for all proplyds. However, they *assume* that the warm ($\simeq 1000$ K) photodissociated gas will be able to flow freely away from the disk at its sound speed ($\simeq 2.5$ km s $^{-1}$), but this is not necessarily the case.

If one allows, for the sake of argument, that a free-flowing photodissociated wind, with a density at its base of $10^6 n_{n,6}$ cm $^{-3}$, is initially established, then, once the ionizing radiation from θ^1 Ori C is switched on, an R-type ionization front will be driven rapidly into the flow. For proplyds closer than

$$d'_{17} \simeq 0.55 n_{n,6}^{-1} r_{15}^{-1/2} \dot{S}_{49}^{1/2}, \quad (10)$$

the flow will be immediately ionized all the way down to the disk. For proplyds further away, the ionization front undergoes a transition to D-

type some way out from the disk, at which point its progress will slow and it will begin to drive a shock into the atomic flow. The density of newly ionized gas n_0 will adjust itself to that given by equations 1 and 4 of §2, but with r_d replaced by the radius of the ionization front. The pressure of the ionized gas will be roughly 20 times that of neutral gas of the same density, so that for proplyds closer than

$$d''_{17} \simeq 20 n_{n,6}^{-1} r_{15}^{-1/2} \dot{S}_{49}^{1/2}, \quad (11)$$

the shock will reach the surface of the disk before stalling, hence quenching the neutral flow in a time of 30–500 years. In proplyds farther away than d''_{17} from θ^1 Ori C, the shock will stall at a distance $z_0 r_d$ from the disk, where

$$1 + z_0 \simeq 0.136 n_{n,6}^{2/3} d_{17}^{2/3} r_{15}^{1/3} \dot{S}_{49}^{-1/3}. \quad (12)$$

The chief uncertainty in the estimates of d'_{17} and d''_{17} is the density at the base of the neutral flow. However, taking the parameters of HST 10 (Johnstone et al., 1996), $r_{15} = 1.3$, $z_0 = 2.3$, $d_{17} = 5$, and assuming $n_{n,6}$ is the same for all proplyds, one finds that $d'_{17} \simeq 0.03 r_{15}^{-1/2}$ and $d''_{17} \simeq r_{15}^{-1/2}$. No proplyds are observed with $d_{17} < d'_{17}$ but a substantial fraction have $d_{17} < d''_{17}$, although the exact number depends on the distribution of disk radii. This can only be determined directly for the dark silhouette disks (McCaughrean and O'Dell, 1996), which show $r_{15} = 0.4$ – 7.6 , but the bright proplyds are likely to have smaller disks ($r_{15} \simeq 0.1$ – 1.0 , Henney et al., 1996; Johnstone et al., 1996). Hence, roughly half of all bright proplyds will **not** have an extended neutral evaporated flow.

The real situation is undoubtedly much more complicated than portrayed above (c.f. Bertoldi and Draine, 1996), but the basic argument, that the neutral flow must have a higher pressure than the overlying ionized flow in order to exist, should remain valid. A further problem for the neutral flow is gravity: the escape speed from the circumstellar disk will equal the sound speed in the neutral gas at a disk radius of $r_{\text{esc},15} \simeq 2.1 M_\star$, where M_\star is the mass of the central star in solar masses ($\simeq 0.1$ – 2 , McCaughrean and Stauffer, 1994). Hence, except for the proplyds with the lowest mass central stars, gravity will dominate the dynamics of the photodissociated region.

Note that the argument against radiation pressure in §2 applies a fortiori to a neutral photodissociated flow since its pressure would have to be larger than the ionized flow. However, the confinement problem could be circumvented if it were maintained that the material in the tail, instead of having been redirected from an initial flow towards θ^1 Ori C, was instead part of a flow from the back side of the disk, possibly driven by the diffuse radiation field. This could also explain the absorption seen in the core of

some tails, but whether the flow would be dense enough for this is not clear. Alternatively, the tails could be formed from the remnants of a dense slow wind from a massive star (Sutherland et al., 1997).

In conclusion, the two-wind interaction model has had qualified success in explaining the observed properties of the proplyds closer to θ^1 Ori C. Various discrepancies remain, however, and further work is necessary both in extending this model and in developing alternatives.

Acknowledgements: We are very grateful to Alex Raga, Susana Lizano and John Meaburn for their contributions to the work discussed in this paper. WJH also acknowledges useful discussions with John Dyson, Dave Hollenbach, Mark McCaughrean and Bob O'Dell. Financial support for this research has been provided by DGAPA-UNAM under project number IN105295 and by Cray Research, Inc.

References

- Bally, J., Devine, D. and Sutherland, R. 1995, In: S. Lizano and J. M. Torrelles (eds.): *Circumstellar Disks, Outflows and Star Formation*, RMAA (Serie de Conferencias) 1, 19
- Bertoldi, F. 1989, ApJ 346, 735
- Bertoldi, F. and Draine, B. T. 1996, ApJ 458, 222
- Churchwell, E., Felli, M., Wood, D. O. S. and Massi, M. 1987, ApJ 321, 516
- Dyson, J. E. 1968, Ap&SS 1, 388
- Felli, M., Taylor, G. B., Catarzi, M., Churchwell, E. and Kurtz, S. 1993, A&AS 101, 207
- Garay, G., Moran, J. M. and Reid, M. J. 1987, ApJ 314, 535
- Hayward, T. L., Houck, J. R. and Miles, J. W. 1994, ApJ 433, 157
- Henney, W. J. and Arthur, S. J. 1997, in preparation
- Henney, W. J., Meaburn, J., Raga, A. C. and Massey, R. 1997, A&A in press
- Henney, W. J., Raga, A. C., Lizano, S. and Curiel, S. 1996, ApJ 465, 216
- Howarth, I. D. and Prinja, R. K. 1989, ApJS 69, 527
- Johnstone, D., Hollenbach, D., Storzer, H., Bally, J. and Sutherland, R. 1996, BAAS 189, 4912 (Available at <http://www.cita.utoronto.ca/~johnston/orion/abstract.html>)
- Kahn, F. D. 1969, Physica 41, 172
- Laques, P. and Vidal, J. L. 1979, A&A 73, 97
- Massey, R. M. and Meaburn, J. 1993, MNRAS 262, L48
- Massey, R. M. and Meaburn, J. 1995, MNRAS 273, 615
- McCaughrean, M. J. 1997, this volume
- McCaughrean, M. J. and O'Dell, C. R. 1996, AJ, 111, 1977
- McCaughrean, M. J. and Stauffer, J. R. 1994, AJ, 108, 1382
- McCullough, P. R., Fugate, R. Q., Christou, J. C., Ellerbroek, B. L., Higgins, C. H., Spinhirne, J. M., Cleis, R. A. and Moroney, J. F. 1995, ApJ 438, 394
- Meaburn, J. 1988, MNRAS 233, 791.
- O'Dell, C. R. and Wen, Z. 1994, ApJ 436, 194
- O'Dell, C. R., Wen, Z. and Hu, X. 1993, ApJ 410, 696
- O'Dell, C. R. and Wong, S. K. 1996, AJ 111, 8460
- Panagia, N. 1973, AJ 78, 929
- Sutherland, R. S., Hartquist, T. W., Bally, J. and Dyson, J. E. 1997, in preparation